M. Hoheisel et al., Journal of Non-Crystalline Solids 227 - 230 (1998) p. 1300 - 1305

Amorphous silicon X-ray detectors

M. Hoheisel[*§], M. Arques[+#], J. Chabbal[+], C. Chaussat[+], T. Ducourant[+], G. Hahm[*], H. Horbaschek[*], R. Schulz[*], M. Spahn[*]

** Siemens AG, Medical Engineering, Basic Development, P.O.Box 3260, 91050 Erlangen, Germany*

+ Trixell, Z.I. Centr'Alp, 38430 Moirans, France

Abstract

Solid-state X-ray detectors are qualified to replace the conventional diagnostic X-ray image intensifier television systems, film-screen, and storage phosphor systems. Such a detector consists of a scintillator layer coupled to a photodiode matrix. Amorphous silicon (a-Si) has proven to be the most suitable semiconductor for such large-area devices. Our detector prototype with a pixel pitch of 200 μm and an active area of 20×20 cm^2 uses one PIN photodiode and one PIN switching diode per pixel for readout. Cesium iodide is used as scintillator.

Evaluation of the detector was performed in the laboratory as well as in a clinical site where it was integrated in a C-arm for cardiological investigations. In this paper MTF, dynamic behavior, noise figures, and quantum yield will be discussed in detail. The outstanding detector performance represents a first step towards the goal of replacing existing fluoroscopic or radiographic X-ray systems for medical diagnosis.

1. Introduction

Medical diagnosis calls for devices which convert X-ray images, i.e. spatial distributions of X-ray intensity after passing the body to be examined, into visible images. The systems should enable the acquisition of single images, image sequences, or even real-time display. Currently, both analog and digital systems are in use. This paper will restrict itself to projection systems, excluding computed tomography.

The traditional analog system is the film-screen combination which yields single images. A film is sandwiched between two scintillating screens. The latter convert X-rays into visible light which exposes the film. Another option consists in taking image sequences by a film camera from the output screen of an X-ray image intensifier (XRII).

Single digital images can be obtained by a storage phosphor plate which subsequently is read out by a laser scan or by an electrostatically probed selenium drum [1]. The combination of an XRII with a TV camera enables real-time imaging.

Most conventional systems suffer from several drawbacks:

- the X-ray dose required is still too high (i.e. the detective quantum efficiency (DQE) is too low),
- an improved spatial resolution especially over large image areas is desirable in some cases,
- XRIIs show geometrical distortions which disturb the periphery of the image, and

§ Corresponding author. Tel.: +49 9131 84-6657; fax: +49 9131 84-4771; e-mail: martin.hoheisel@med.siemens.de

now with: LETI, Grenoble, France

- detector weight and bulky geometrical dimensions rule out a lean system.

Therefore, solid state detectors based on amorphous silicon (a-Si) are under development [2][3][4][5]. The operating principle is fairly simple: an input screen consisting of CsI as a scintillator converts X-ray quanta into visible photons. These photons are transformed to discrete charge distributions by a matrix of a-Si photodiodes which subsequently are read out.

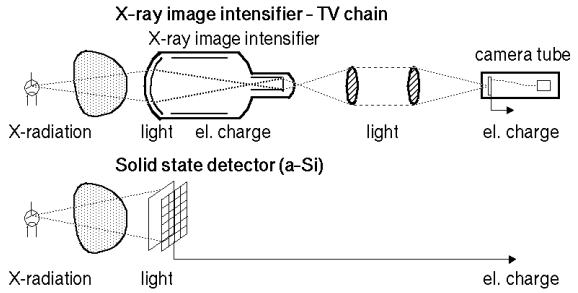

Fig. 1. Comparison between XRII-TV chain and a-Si solid state detector.

On the contrary, the conventional XRII-TV chain requires a great number of conversion steps (Fig. 1): In the first step absorbed X-ray quanta are converted to photons in the visible range, which in their turn are converted to electrons. The electrons are accelerated towards the output screen where they generate visible light. This light is projected via an optical system onto a video camera where the photons are again transformed to charge carriers which are scanned by the electron beam.

Hence, the requirements to realize an a-Si X-ray detector are a large area scintillator and a large area semiconductor. Optimal performance is obtained by CsI doped with Tl and plasma-deposited hydrogenated amorphous silicon which can be both easily deposited on areas required to examine human bodies (20 - 50 cm).

The well-known advantages of a-Si are its low deposition temperature (200 - 250°C) which permits the use of nearly arbitrary substrates, its ample semiconductor properties (photoconductivity in the visible spectral range, field effect), its compatibility with silicon process technology, and of course its good stability against X-ray radiation.

A degradation by prolonged illumination (Staebler-Wronski effect [6]) is not observed since the photodiodes are operated under reverse bias, and the light intensities are several orders of magnitude lower than those applied to solar cells.

X-ray detectors can also use other absorbers. Fig. 2 shows the calculated DQE at zero spatial frequency for CsI, selenium, and a storage phosphor system.

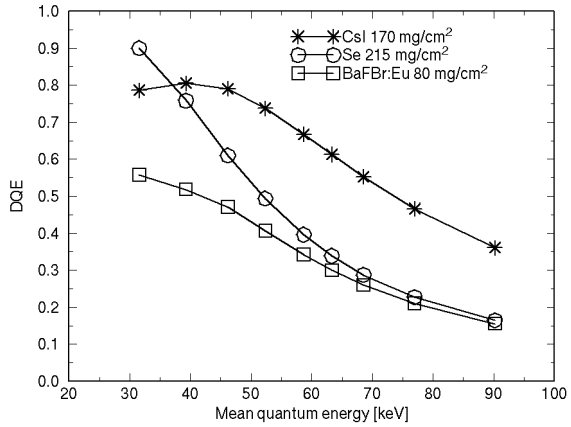

Fig. 2. Detective quantum efficiency (DQE) at zero spatial frequency of three different X-ray converters: scintillator (CsI), direct converter (Se), and storage phosphor (BaFBr:Eu).

The CsI scintillator parameters were chosen as in our detector, i.e. thickness 420 μm. The Se absorber was assumed to be 500 μm thick, which is about the upper limit for state-of-the-art technology [7]. The storage phosphor screen was a 80 mg/cm^2 BaFBr:Eu layer. The X-ray spectra were DN2 - DN10 according to the German standard DIN6872 (40 - 150 kV tube voltage, 4 - 47.5 mm thick Al filter).

Since standard investigations (abdomen, scull, card) are carried out at 70 - 80 kV and thorax images are taken at about 120 kV, Fig. 2 reveals clearly the superiority of CsI. Only at very low energies which are commonly used for extremities (hands, feet) Se performance is comparable.

2. Detector Design and Technology

The detector consists of a 450 μm thick CsI:Tl layer coupled to the a-Si panel (Fig. 3). A matrix of 1024 × 1024 pixels is built on a glass substrate resulting in an active area of 20 × 20 cm^2. Each pixel

with 196 × 196 μm^2 in size is connected to a column line for readout and a row line to apply driving voltages. The diodes can be optically reset by light flashes applied from the bottom of the photodiodes through the substrate. The detector is completed by driving and readout electronics, analog-to-digital converters, a programmable timing generator, and a system board with optical fiber communication to the host computer.

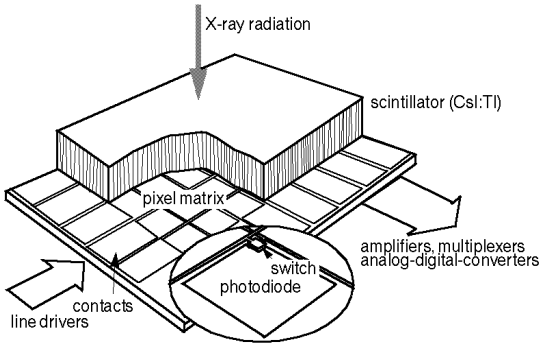

Fig. 3. Schematic drawing of an a-Si X-ray detector panel.

A second type of detector panel has been built with 143 × 143 μm^2 pixels. This leads to a reduced image area of only 14.6 × 14.6 cm^2, but with a higher spatial resolution. This sample was used for radiological investigations.

Every pixel consists of a NIP photodiode and a PIN switching diode (Fig. 4). Compared to using thin-film transistors (TFTs), this double diode technology is easier to produce and has the advantage of an improved geometrical fill factor. The fill factor is defined as the percentage of photodiode area with respect to the total pixel area, in our case 70% and 67% for the 196 μm and the 143 μm panel, respectively.

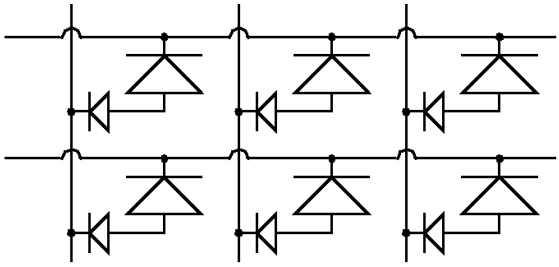

Fig. 4. Pixel structure of the double diode technology. The row lines are for driving voltage pulses, the column lines are for charge readout.

Both diodes are made from hydrogenated a-Si deposited by a conventional plasma-enhanced CVD process. The photodiodes are optimized for low dark current density (< 1 nA/cm^2 at -4 V) and high quantum efficiency in the visible spectral range (> 80% at 550 nm). The capacity of one photodiode is 1.9 pF.

The switching diodes are designed to be as small as possible (20 × 20 μm^2). Their leakage current density is 10 nA/cm^2 at a bias of about -4 V. To permit high forward currents, they exhibit an ideality factor n_s = 1.8 and a low series resistance.

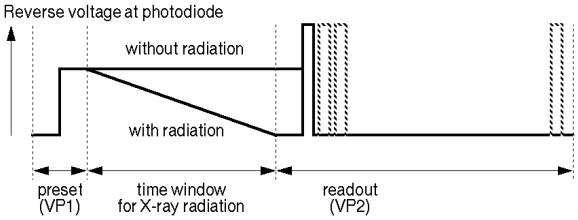

Fig. 5. Frame timing of the double diode detector panel. The reset light is included in the preset phase.

The timing diagram of one readout frame is depicted in Fig. 5: a first voltage pulse VP1 (typically ≈ -4 V) is simultaneously applied to all photodiodes of the whole panel and biases them in reverse.

Then a time interval of several milliseconds is retained where the X-ray tube can be switched on. Depending on the local dose incident on the detector, light and accordingly charges are generated in the photodiodes resulting in a voltage drop.

Subsequently, a second voltage pulse VP2 (≈ -4.5 V) is applied row by row, charging the diodes to a somewhat higher voltage. The charge needed is read out via the column lines and fed to a custom designed readout amplifier. The collected charge is a measure for the incident X-ray intensity.

The final step is a short back-side illumination of the panel. This reset light flash decharges all diodes and fills the deep traps in the a-Si to ensure identical starting conditions for all diodes in the next frame. The reset light intensity has to be optimized carefully to guarantee a trap occupancy which is able to reduce markedly the so-called memory effect (see below).

A certain difficulty occurs because it is impossible to charge a capacitor in a short time through a diode like in the case of a resistor. No exponential behavior with a fixed RC time constant is observed, but a much slower course. This leads to a poor linearity at low signals. Reproducible results can only be obtained with a voltage pulse VP2 > VP1 which results in an additional offset charge. This charge is subtracted later on during the correction procedure.

The readout circuits have 120 charge sensitive input channels with several switchable sensitivity ranges, sample-and-hold circuits, and an output multiplexer. After amplification the signal is digitized with 12 bit resolution. A fast image processor (input data rate > 25 MB/s) permits subtraction of dark images, correction of individual pixel gain, and repair of defective pixels by interpolation from their neighbor pixels in real-time.

3. Detector Performance

The detector is operated basically in two different modes:

- fluoroscopy to examine the patient in real-time for a longer period (up to several minutes), and
- radiography to acquire single images.

In fluoroscopy mode a very low X-ray dose is mandatory. The system dose, i.e. the average dose over a region of interest, is typically 15 nGy per image with a frame rate of 12.5 Hz (1024 × 1024 matrix) or 25 Hz (512 × 512 matrix).

The system dose for radiography is in the order of ≈ 1 μGy. This dose is considerably lower than the dose required for conventional film-screen combinations. Using a typical sensitivity (film-screen sensitivity class 400), 2.5 μGy are required.

Sensitivity measurements were performed with 70 kV tube voltage and 21 mm aluminum beam filtration [8]. This leads to an X-ray spectrum which is close to those used in standard medical investigations. The detector sensitivity (= the average number of electrons which are read out per X-ray quantum incident on the detector surface) was determined to be 1150 e^-/X_{inc}. Taking into account X-ray absorption and fill factor, this value is equivalent to a photo-electric sensitivity (= the number of electrons which are generated in the photodiode per X-ray quantum absorbed in the scintillator on the area of the corresponding photodiode) of 2400 e^-/X_{abs}.

Key parameters for image quality are the DQE, the spatial resolution expressed by the modulation transfer function (MTF), linearity, image lag, coarse contrast ratio, and long term stability. The DQE is the most important quantity to characterize the performance of X-ray detectors since it is a measure for contrast detail detectability and dose requirement. Beside X-ray absorption, electronic noise contributions mainly determine the DQE at low dose.

Fig. 6 shows the measured dependencies of the DQE on spatial frequency for different doses. In the case of radiography (high dose), signal and quantum noise are large compared to the electronic noise. Thus the DQE at low spatial frequencies reaches the value of X-ray absorption which is nearly 0.7 under DN5 conditions [8].

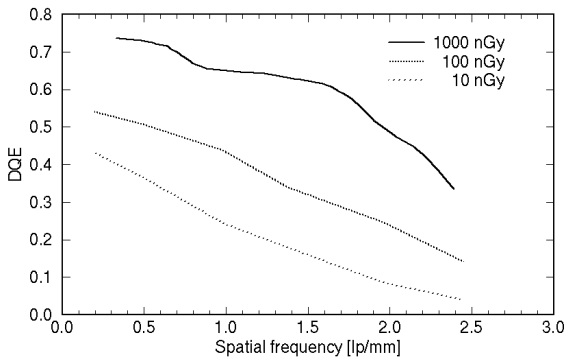

Fig. 6. Detective quantum efficiency (DQE) of the a-Si detector at different doses.

With reduced dose, the DQE decreases markedly because electronic noise exceeds quantum noise thus becoming dominant in the total noise. That means that the image quality is reduced mainly by electronic noise. Accordingly, fluoroscopy is the most demanding mode for the a-Si detector.

Therefore, special emphasis has been laid on the study of the different noise sources. The total electronic noise level with respect to the a-Si panel output amounts to 1450 e^-. This noise is composed of the following contributions:

- pixel noise which comes from the photodiode reset and amounts to ≈ 750 e^- (depending on the photodiode capacitance C_P and the switching diode ideality factor n_s),

- shot noise originating from leakage currents (< 250 e^-),
- emission of charge carriers from traps in the a-Si bulk of the switching diodes (≈ 400 e^-), and
- the readout circuits. The samples in use for this study deliver a noise of ≈ 1010 e^- operated with an input load of 115 pF (column line capacitance, connectors). With the next generation of readout circuits this noise will be reduced considerably.
- Minor noise sources are line resistances, the analog chain, and the AD converter.

MTF is beside DQE crucial for small detail detectability. It is determined by the spatial resolution of the scintillator and the size of the photodiodes. The light output of the CsI layer is enhanced by a white reflector on the back side which, however, deteriorates resolution.

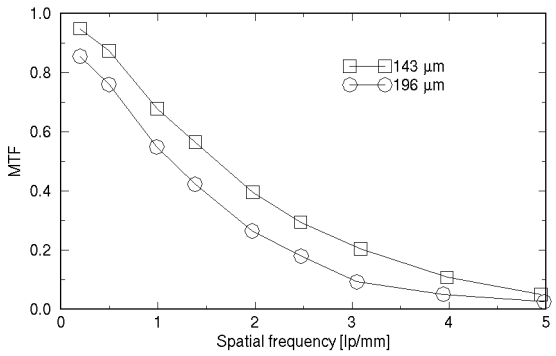

Fig. 7. Modulation transfer functions (MTF) of two a-Si detectors with different pixel pitches.

Fig. 7 shows the outstanding MTF of the two detectors with 196 µm and 143 µm pixel pitch. The MTF at 2 lp/mm amounts to 0.39 for the 143 µm detector. Due to the excellent MTF of the CsI scintillator, this value is much higher than even the MTF of a detector with 127 µm pixels [9]. The latter amounts to 0.24. It should be pointed out that even near the Nyquist frequencies which are 2.55 and 3.5 line pairs per mm for the two types of detectors, the MTF is still as high as 0.18. As a matter of fact, this good MTF can lead to aliasing effects.

Since the photodiodes are operated under reverse bias, the photocurrents are of primary nature [10]. Therefore, a good linearity behavior is expected. At -4 V, errors of 0.3% were observed. Other linearity aberrations in the order of ≈ 1% originate from the readout circuits.

The time response behavior of the detector is crucial for practical applications. Single images must not show ghost images of former investigations. Real-time fluoroscopy has to be free from image lag. This is particularly important when high dose images have been acquired a short time before.

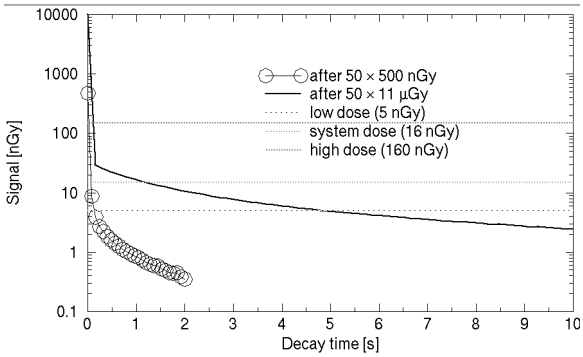

Fig. 8. Signal decay of the a-Si detector in fluoroscopy mode after application of 50 X-ray pulses of 500 nGy or 11 µGy. The dotted lines show the system dose and the dose in bright and dark image areas, for orientation.

Fig. 8 shows the signal decay in fluoroscopy mode. After taking 50 images with 3 times the maximum dose (i.e. 500 nGy), the amplitude of a residual image in the following frame is < 2%. The more critical case is high dose exposure. 50 X-ray pulses of 11 µGy had been applied (system dose for radiographs is 2.5 µGy, for instance). Then a long-term decay could be observed. Compared to the dose situation in fluoroscopy, the residual signal equals the signal of the system dose after 1.2 s. It takes 5 s until the residual signal is lower than the signal in the darkest parts of the image.

The origin of this lag is mainly deep trapping and emission of electrons from traps in the a-Si diodes [11]. But CsI:Tl is also known to show some afterglow. This topic is currently under investigation.

The coarse contrast ratio is the image signal ratio between the signal behind a large area of a totally absorbing object (e.g. a lead disk) and the maximum signal. Values of > 1:100 are reached which are considerably larger than those of the XRII-TV chain (≈ 1:20 - 1:30).

Long term stability of the a-Si detector seems to be no major problem. After application of a lifetime X-ray dose (≈ 80 Gy), only a slight increase in dark offset was observed. Since the offset is acquired

permanently during stand-by, such an increase or little drifts due to temperature changes are subtracted automatically.

4. Conclusions

The a-Si detector exhibits all properties which are required for medical X-ray diagnosis. Therefore, a sample of our detector has been tested in a clinical laboratory for more than one year. Over 200 patients have undergone cardiac investigations. The results demonstrate the outstanding image quality especially at higher dose (digital cinema mode).

On the other hand, the signal-to-noise ratio at low dose (fluoroscopy) still has to be improved. This will be accomplished by advanced design rules for the a-Si panel itself, improved process technology, and the next generation of readout circuits.

The second detector with 143 μm pixel pitch was tested in another clinical site with respect to its usefulness for radiological applications. It exhibited an excellent image quality with system doses as low as 2.5 μGy, 1.25 μGy, and 625 nGy, corresponding to a film-screen combination sensitivity classes of 400, 800, and 1600, respectively.

In summary, the following advantages of the a-Si detector should be pointed out:

- flatness and compactness, lighter and more handy system
- no geometrical distortions at the edges
- insensitive to magnetic fields (earth magnetic field or MR devices in the vicinity)
- homogeneous resolution and sensitivity over the whole image area
- excellent large area (coarse) contrast compared to XRII-TV systems
- high sensitivity and consequently possible dose reduction
- real-time radiography (no film processing, no cassette handling)
- no optics, no vacuum, no chemicals
- direct image transfer to PACS (Picture Archiving and Communication System)
- mixed fluoroscopic and radiographic applications with one system feasible.

Our work has furnished evidence for the usefulness of the detector concept and the excellent performance. Hence, a first milestone was reached towards the goal of replacing existing fluoroscopic (XRII-TV) and radiographic (storage phosphor) systems for medical diagnosis.

Acknowledgments

The project was also advanced by numerous co-workers at Thomson Tubes Electroniques. The contributions of D. Hassler, G. Schmidt, H. Schreiner, K. Stierstorfer and many others of Siemens Medical Engineering are gratefully acknowledged.

This work was supported in part by EUREKA grant EU 651 under the name ASTRID (Amorphous Silicon Technology for Radiographic Image Diagnostic) and by the French Department of Industry.

References

[1] U. Neitzel, I. Maack, S. Günther-Kohfahl, Med. Phys. 21 (1994) 509
[2] J. Chabbal, C. Chaussat, T. Ducourant, L. Fritsch, J. Michailos, V. Spinnler, G. Vieux, M. Arques, G. Hahm, M. Hoheisel, H. Horbaschek, R. Schulz, M. Spahn, Proc. of SPIE 2708 Physics of Medical Imaging (1996) 499
[3] T. Graeve, Y. Li, A. Fabans, W. Huang, Proc. of SPIE 2708 Physics of Medical Imaging (1996) 494
[4] U. Schiebel, N. Conrads, N. Jung, M. Weibrecht, H. Wieczorek, T. Zaengel, M. J. Powell, I. D. French, C. Glasse, Proc. of SPIE 2163 Physics of Medical Imaging (1994) 129
[5] L. E. Antonuk, J. Yorkston, W. Huang, J. Boudry, E. J. Morton, R. A. Street, Proc. of SPIE 1896 Physics of Medical Imaging (1993) 18
[6] D. L. Staebler, C. R. Wronski, Appl. Phys. Lett. 31 (1977) 292
[7] D. L. Lee, L. K. Cheung, L. S. Jeromin, E. F. Palecki, B. Rodricks, Proc. of SPIE 3032 Physics of Medical Imaging (1997) 88
[8] equivalent to DN5 defined in German Standard DIN6872
[9] L. E. Antonuk, Y. El-Mohri, W. Huang, K. W. Jee, M. Maolinbay, V. E. Scarpine, J. H. Siewerdsen, M. Verma, J. Yorkston, Proc. of SPIE 3032 Physics of Medical Imaging (1997) 2
[10] M. Hoheisel, G. Brunst, H. Wieczorek, J. Non-Cryst. Solids 90 (1987) 243
[11] H. Wieczorek, J. Non-Cryst. Solids 164-166 (1993) 781